Desalination and Water Treatment
www.deswater.com

doi: 10.5004/dwt.2017.1809

58 (2017) 154–167
January

Removal of lead, copper and cadmium ions from aqueous solution using raw and thermally modified diatomite

Eda Gokirmak Sogut[a], Necla Caliskan[b,*]

[a]*Van Security Vocational School, Yüzüncü Yıl University, 65080, Van, Turkey*
[b]*Department of Physical Chemistry, Faculty of Science, Yüzüncü Yıl University, 65080, Van, Turkey, Tel. +90 432 2251024/2283; Fax: +90-432-225-1256; email: ncaliskan7@hotmail.com*

Received 25 December 2015; Accepted 13 June 2016

ABSTRACT

In this study, raw diatomite was purified by thermal treatment in order to improve the adsorption capacity of diatomite. The prepared calcined diatomite samples were characterized by the X-ray diffraction (XRD), scanning electron microscope (SEM) and Fourier transformation infrared (FT-IR) analysis techniques. The raw and thermally modified diatomite at 500°Cwas tested for the adsorption of Pb(II), Cu(II) and Cd(II) from aqueous solutions. Adsorption experiments were performed under batch process, using metal ions initial concentration, contact time and temperature as variables. The linear Langmuir, Freundlich and Dubinin–Radushkevich (D–R) adsorption equations were applied to describe the equilibrium isotherms. Equilibrium studies showed that thermally modified diatomite has a higher removal capacity for Pb(II), Cu(II) and Cd(II) from water than untreated diatomite. The kinetic data were evaluated using the pseudo-first-order, pseudo-second-order and intraparticle diffusion kinetic equations. The experimental data proved a closer fit to the pseudo-second-order model. Thermodynamic parameters such as the enthalpy (ΔH^0), Gibbs' free energy (ΔG^0) and entropy (ΔS^0) were calculated for raw and thermally modified diatomite. These values showed that the adsorption of Pb(II), Cu(II) and Cd(II) ions onto diatomite samples was controlled by a physical mechanism and occurred spontaneously.

Keywords: Diatomite; Thermal treatment; Heavy metals; Adsorption; Kinetics

1. Introduction

Diatomite ($SiO_2.nH_2O$) or diatomaceous earth of high porosity (80%–90% voids), low density, large specific surface area, chemical stability, thermal conductivity and fine particle size (10–200 μm) is sedimentary rock composed of hydrated silica microfossils shells of the single-cell algae, generally known as diatoms. The structure of these diatoms formed mainly of silica [1,2]. In addition, the siliceous skeleton may include small amounts of organic [3] and inorganic components such as alumina mainly and lesser amounts of iron, alkaline earth, alkali metals, carbonates and other minor constituents [4]. It has plentiful surface hydroxyl functional groups (S–OH) and structural negative charge which arises from isomorphic substitution of Al^{3+} and/or Fe^{3+} for Si^{4+} in the crystal lattice [5]. Although diatomaceous earth contains a large number of different binding sites such as silanol (Si–OH), aluminol (Al-OH), titanol (Ti–OH), and iron hydroxyl (Fe–OH), only the presence of the dominant surface sites such as silanol and/or aluminol is assumed. This assumption is made to make simpler the fitting calculation of equilibrium constants. Hydroxyl groups act as centers for adsorption through forming hydrogen bonds with the adsorbate [6] and can be divided into isolated free silanol (–SiOH), geminal free silanol ($-Si(OH)_2$), and vicinal or bridged or OH groups bound through the hydrogen bond [7]. And also, diatomite consists of siloxane groups or –Si–O–Si– bridges with oxygen atoms on the surface [8]. Diatomite is used as filtration media for various beverages [1,9], building material [10], catalytic matrix [11] and pozzolanic additive [12].

* Corresponding author.

In addition, diatomite as adsorbent is widely used in the removal of heavy metal ions [13,14]. The increasing concern about the pollution of the natural environment has encouraged growing attention in the existence and behavior of heavy metals in soils and water [15]. Lead and its compounds are considered as toxic pollutants and are included in the water hazard class 2. Copper is one of the biologically essential ions but is only required at low concentrations. Concentrations of copper higher than 1.0–1.5 mg L^{-1} in water lead to ecological and health problems. Cadmium is known for its toxicity with serious implications on human health [16].

The use of diatomite as adsorbent, in addition to mineralogical composition of the material, depends on the physicochemical properties such as the adsorption capacity, surface area, pore volume and surface charge. The natural form of diatomite is modified with the purpose of get better its physicochemical properties. Thermal treatment is one of these modification methods and changes structures of diatomite (temperature below the melting temperature). Recently, some studies have been presented on thermally modified diatomite as effective adsorbent for removing textile dyes and heavy metals from water solutions [1,4, 17,18]. Before thermal treatment diatom-silica presents a high hydrated surface, in which most of silanols are covered with H-bonded water [19]. Generally, an increase in thermal treatment has an important effect on the type, distribution and content of surface hydrated species (water, H-bonded silanols and isolated silanols), affecting key reactive sites for different surface reactions, with its adsorption capability [4]. The raw diatomite contains organic impurities, which are removed after the calcinations [17]. Organic materials and carbonates decompose to CO_2 and SO_2 gases plus H_2O and leave the bulk of diatomite during the thermal operation [3]. The removal of impurities leads to reduction of the specific surface area and increases the average pore diameter of raw diatomite, and also improves its adsorption capability of heavy metals and dyes [17]. Besides, high temperatures cause damage of vicinal micropores walls, which lead to a decrease in micropore and a corresponding increase in mesopore content [18]. The mesopores have the most influence in the adsorption of pollution which enables their surfaces to be accessible to solute molecules or ions [8].

Southeast of the central Anatolia and western Anatolia regions have the main source of diatomite in Turkey. It has recently been found to be the source of diatomite in the eastern region of Anatolia. In addition, a license area is available in Van. Diatomite is an inexpensive material. However, the cost of diatomite depends on its quality, how it will be used, and the preparation effort that has been invested by the supplier. The cost of diatomite that is straight from the mine without processing for use in industry starts at about $7 per ton. In this study, diatomite sample was collected from the area of southern Caldiran district in the province of Van (Eastern Turkey). Raw diatomite was calcined in order to improve the adsorption capacity of diatomite. Therefore, natural diatomite, which is a low-cost material, was modified by thermal process at different temperatures (100–1,000°C intervals) As a result of the evaluation of literature data and diatomite characterization analyzes (mineralogy and surface properties etc.), the thermal processing temperature was selected as 500°C for modification. The effects of thermal treatment on adsorption of Pb(II), Cu(II) and Cd(II) ions onto diatomite have been examined, and the optimum conditions have been determined for the maximum adsorption of these ions from aqueous solutions. The nature of the adsorption process has been also evaluated according to its kinetics, isotherms and thermodynamic aspects.

2. Experimental

2.1. Preparation of absorbent materials

The collected material from Caldiran-Van region, was washed once with distilled water and then dried at 105°C for 24 h, desiccated and sieved through 350 mesh sieve. Quantitative chemical analysis of diatomite obtained by X-ray fluorescence (XRF) technique revealed that the Caldiran-Van diatomite consists mainly of SiO_2 (69.70%), and it has 11.50% Al_2O_3, 4.40% Fe_2O_3, 0.65% TiO_2, 0.80% Na_2O, 1.40% K_2O and 11.55% loss on ignition [20]. The prepared sample was thermally treated under different calcining conditions. For thermal treatment of diatomite, samples, each having a mass of 10 g, were heated to 1,000°C in 100°C intervals at a rate of 10 K/min and were thermally treated by keeping at each temperature for 2 h in a furnace. Thermal treatment time of diatomite was selected as 2 h because specific surface area did not change significantly with time [21], that is why it was kept constant above this time. Samples were then labeled as D_{100}, D_{200}, D_{300} and so on, and stored in polyethylene bags. Thermally untreated sample marked as D_R. During the experimental procedure, 11 different diatomite samples were obtained and evaluated in total [4].

2.2. Sample characterization

XRF spectrometer (Philips 2400) was used for chemical composition analysis of diatomite sample. Thermogravimetric (TG) and Differential Thermal Analysis (DTA) was performed using Rigaku 2.22E1 Thermal Analyzer under the following operational conditions: heating from 10°C to 1,099°C at a rate of 20°C min^{-1} in atmospheric air. The specific surface areas (S) of each sample were determined by the Brunauer–Emmett–Teller (BET) procedure by using N_2 adsorption data. Fourier-transform infrared (FT-IR) measurement was mounted on a Bio-Rad Win-IR spectrometer at a resolution of 2 cm^{-1} in KBr pellet at room temperature. The infrared spectra of prepared samples between 400 and 4,000 cm^{-1} were recorded. For mineralogical analysis, X-ray diffraction (XRD) pattern of diatomite were recorded by a Philips PW 1830-40 X-ray diffractometer with a Cu-K radiation. The morphology of samples was examined by a scanning electron microscopy (SEM; model: LEO 440 computer controlled digital) [20]. The pH values of the raw and thermally modified diatomite suspensions were determined by a WTW pH meter (Series 720, Germany).

2.3. Preparation of heavy metal standard solutions

All the chemicals employed were analytically pure, and experiments were conducted using Pb(II), Cu(II) and Cd(II) salt solutions. For this purpose, a stock solution containing 1,000 mg L^{-1} of Pb(II), Cu(II) and Cd(II) ions was prepared by dissolving the appropriate amount of nitrate salts (Merck) in 1 L of doubly distilled water.

2.4. Determination of the point of the zero charge (pH_{pzc})

Surface charge density depends on pH of the media. It is well known that surface charge of an adsorbent can be adjusted by altering the pH of the solution according to the pH_{pzc} [22]. The pH_{pzc} for the adsorbents was identified as the pH where 0.1 M HNO_3 titration curves of different adsorbent masses (0.10, 0.20, and 0.30 g suspended in 0.03 M KNO_3) converged with that of the reactive blank solution [20]. When pH value is equal to pH_{pzc}, the surface charge of adsorbents is neutral. At pH values greater than pH_{pzc}, the adsorbent surface becomes negatively charged; it causes more attraction of the Pb(II), Cu(II) and Cd(II) ions onto the surface of adsorbents and increases the adsorption capacity of studied metal ions by the adsorbents [23]. The pH_{pzc} are determined as 3.70 for natural diatomite; thus, its surface may be negatively charged, due to the presence of surface hydroxyl sites, and able to adsorb positively charged heavy metal ions.

2.5. pH of adsorption

The speciation of each of the metals such as lead, copper, cadmium and zinc ions in solution is examined in single- and multi-element systems by Srivastava et al. [15]. According to this paper, Cu^{2+} and Pb^{2+} species occur up to pH ~6.0 in both systems, and cadmium ion exists predominantly as Cd^{2+} species up to pH ~8.0 studied in both the systems. Since at pH range above 6.0 for Cu^{2+} and Pb^{2+} ions, and above 8.0 for Cd^{2+} ion, precipitation occurs in the solutions; the experiments are not conducted beyond these values of pH. Similar trends were reported by other researchers [23]. Therefore, adsorption studies were performed at pH 4.0 because it was the pH > pH_{pzc} which is due to the electrostatic attraction between negative charged groups at the adsorbent surface and the positive charged metal ions.

2.6. Adsorption studies

In this study, sorption potential of Pb(II), Cu(II) and Cd(II) ions was investigated using natural and thermal modified diatomite (D_{500}) as adsorbents in aqueous solutions by batch technique in 10 mL polyethylene tubes. To compare the heavy metal ions adsorption of adsorbents, 0.1 g of raw and calcined diatomite was added into 10 mL of metal ions (Pb^{2+}, Cu^{2+} and Cd^{2+}) solution with different initial concentrations of: 10 mg L^{-1}, 15 mg L^{-1}, 30 mg L^{-1}, 45 mg L^{-1} and 60 mg L^{-1}, and the aqueous solution was shaken in a thermally controlled automatic shaker at temperatures of 298, 308, 318 and 328 K, at 120 rpm for different time periods (1, 5, 10, 15, 20, 30, 45, 60, 90 and 120 min) until equilibrium conditions had been reached. Initial experiments indicated that the time period necessary for equilibrium to be attained in the metal ions/adsorbent systems was 90 min, since after this time the amount of metal ions adsorbed did not alter remarkably with time. Therefore, in all experiments performed, 90 min was selected as the optimum contact time. The remaining ion concentrations in the aqueous solutions after the adsorption process were measured by a Solaar AA M series v1, 23 model (Thermo Scientific, UK) atomic absorption spectrophotometer.

3. Results and discussion

3.1. Thermal treatment of raw diatomite

The properties of pure silica or silica-containing materials such as diatomite, as an oxide adsorbent, are determined in the first step: (i) the porous structure of the material and (ii) the chemical activity of the surface. This activity is related to the concentration and the distribution of different types of OH groups, and on the presence of siloxane bridges [6]. The density of the hydroxyl groups is proportional to the specific surface area. Amorphous silica contains not only OH groups on the surface, but also structurally bound water within the silica structure and inner ultramicropores of the material [6,24]. Firstly, the effects of thermal treatment on specific surface area of diatomite are investigated, and the results are shown in Fig. 1.

Specific surface area of raw diatomite, S_{BET}, increased (from 55.778 m^2 g^{-1} up to 65.902 m^2 g^{-1}) initially with increasing the calcination temperature (room temperature–200°C). Next, it is seen that the specific surface area decreases with increasing thermal process temperature (200°C –400°C). It remains almost constant between 400°C and 600°C (35.438–36.419 m^2 g^{-1}). Similar results of the specific surface area analysis of the diatomite have been reported by Aivalioti et al. (2012) and Reza et al. (2015). Finally, at higher temperatures (~900°C), the specific surface area of the diatomite significantly decreased (down to 3.475 m^2 g^{-1}), indicating important structural changes and possibly a lower potential adsorption capacity [4]. It can be seen that thermal treatment of raw diatomite at 500°C decreases the surface area from 55.778 to 40.296 m^2 g^{-1}. This may be explained by that the organic impurities in raw diatomite have larger surface area than the diatom skeleton, after the organic impurities removed from diatomite by applied thermal process, the surface area and pore volume decrease while the average pore diameter increases [17]. The infrared spectra of the raw and thermally treated diatomite samples (100°C–1,000°C) are given in Fig. 2, and the infrared spectra of the D_R and D_{500} are given in Fig. 3(a, b). It is seen from Fig. 2 that OH groups were removed from the surface after calcinations as the intensity of their absorption, in the high-frequency region, was decreased.

The main absorption bands for D_R, as depicted in Fig. 3, were found at 3,626; 3,394; 1,681; 1,635; 1,475; 1,095; 798; 694 and 466 cm^{-1}. The band at 3,626 is due to the free silanol group (SiO–H), and the band at 1,635 cm^{-1} represents H–O–H

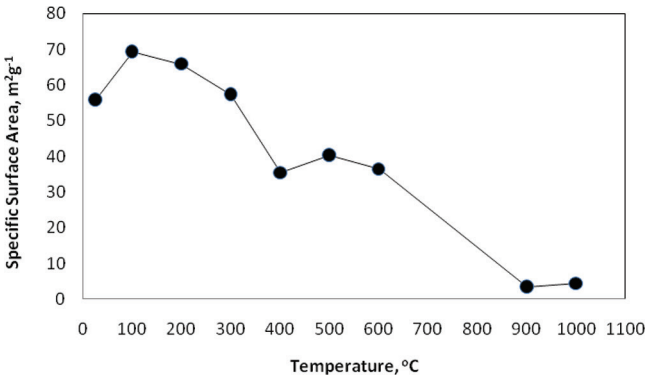

Fig. 1. Variation of specific surface area of diatomite with different thermal treatment temperature.

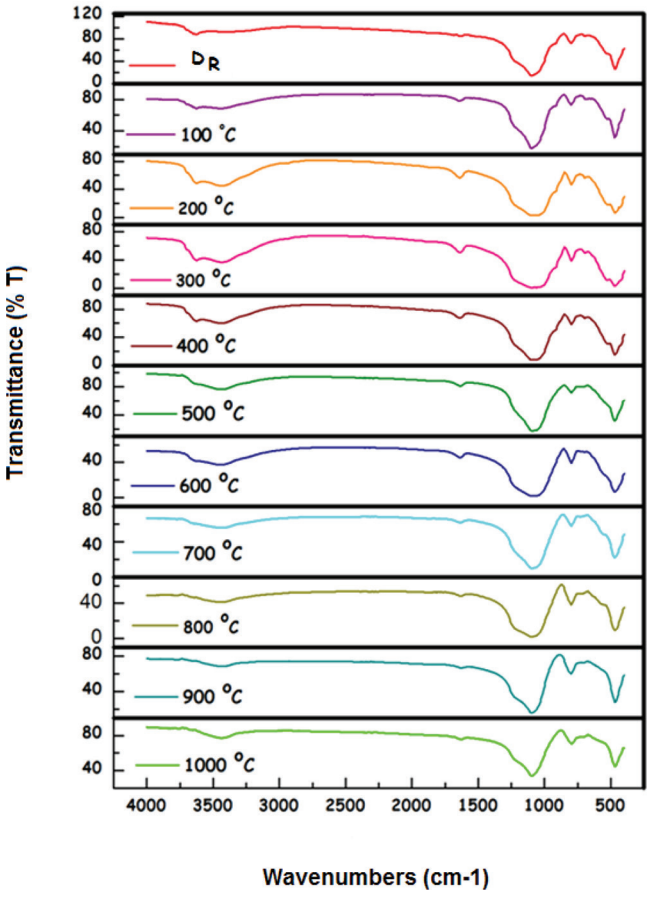

Fig. 2. Infrared spectra of D_R and calcined diatomite at various temperatures.

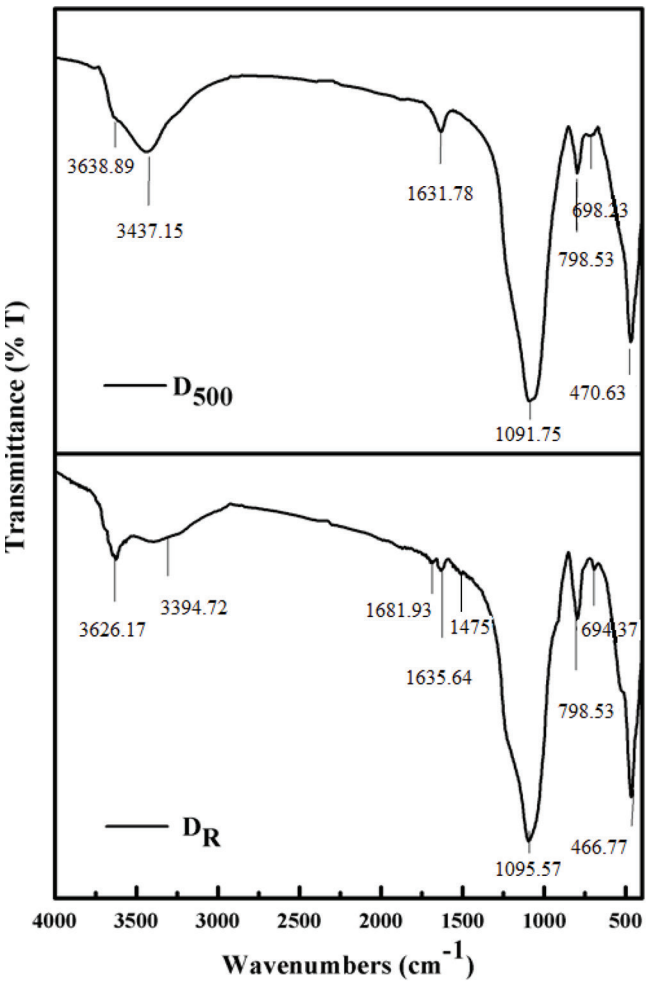

Fig. 3. Infrared spectra of D_R and D_{500}.

bending vibration of water. Hydroxyl groups are either isolated or H-bounded on the surface of diatomite. As a result, the surface is also predominantly covered by weakly adsorbed water in the cavity and water bounded to the surface hydroxyl groups via H-bonds. They can be seen as a wide band with middle wavelength at 3,400–3,500 cm^{-1} [8]. The band at 1,095 may be attributed to siloxane (–Si–O–Si–) group stretching, and the 798 cm^{-1} band represents the stretching vibration of Si–Al–O [25]. The absorption peaks around 694 and 466 cm^{-1} are attributed to the Si–O–Si bending vibration [8]. From the spectrum of calcined diatomite (D_{500}), peaks at 1,091 and 798 cm^{-1} may correspond to (–Si–O–Si–) asymmetry stretching vibration and the (–Si–O–Si–) symmetric stretching vibration peak, respectively [26]. The band at 470 is associated with the (–Si–O–Si–) bending vibration peak. The weak band at about 3,700 cm^{-1} can be attributed to the surface isolated hydroxyl groups bonded to silicon, and the band at 3,638 cm^{-1} is related to the neighboring silanol and hydroxyl groups in the micropore, which is in agreement with the infrared spectroscopic data [27]. Besides, the stretching vibration and the bending vibration of OH functional group were found bands at 3,437 and 1,631 cm^{-1}, respectively [21]. The infrared spectra of D_R reveal that the weak bands of organic compound at 1,475 and 1,681 cm^{-1} of raw diatomite disappear in D_{500}, confirming that the organic impurities were removed from the raw diatomite after calcination [17,28].

The surface of diatomite without thermal treatment, most of isolated silanols and H-bonded ones are H-bonded with capping water molecules. There exist physisorbed water molecules on the ground of the layer of capping water. After calcination treatment, physically adsorbed water is released from the surface and the hydroxyl groups condense [19,29]. At a sufficient concentration hydroxyl groups make such a surface hydrophilic. The OH groups act as the centers of adsorption during their specific interaction with adsorbates. Yaroslavsky using the infrared spectroscopy method has determined for a qualitative temperature course of free isolated OH groups with the maximum at about 500°C [6,30].

TG–DTA curve for the diatomite is shown in Fig. 4. As previously presented [20] for natural diatomite, TG curve exhibits three distinct weight loss steps: (1) between room temperature and ca. 250°C, (2) range from about 250°C–475°C, and (3) in the range of about 475°C–590°C, and the DTA curve shows several endothermic and exothermic peaks. In general quartz is known to give an endothermic reaction between 560°C and 565°C, calcite and dolomite between 690°C and 720°C, kaolinite between 530°C and 590 °C and water between 70°C and 130°C. Conversely, volatile organic compounds give exothermic reactions between 300°C and

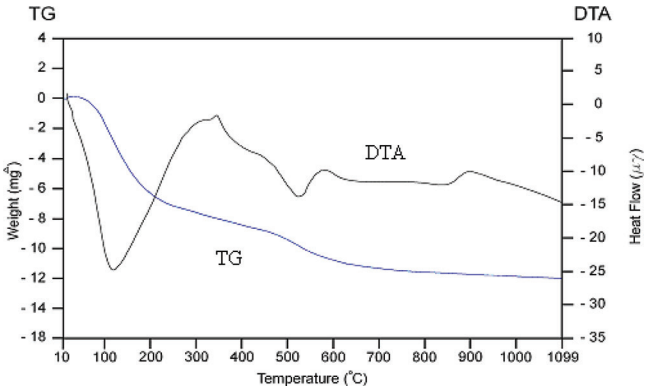

Fig. 4. TG–DTA curve of diatomite sample.

670°C, feldspar and alumina minerals between 780°C and 850°C, kaolinite between 900°C and 1,000°C (transformation into crystalline phases) [31].

In the DTA curve of diatomite, the appearance of the endothermic peak at room temperature and ca. 200°C due to the loss of absorbed water. The related TG curve shows that about 6.2% weight loss was caused. Also in the DTA curve, there is an exothermic peak around 350°C that shows the existence of organic material, though in small amounts [32]. The TG curves show that the weight loss (2.7% between 250°C and 475°C) was caused by the burning of organic material. The next weight loss step of 1.0% between 475°C and 590°C corresponds to the dehydroxylation. The peak at 522.7°C in DTA curve might be due to the liberation of water caused by dehydroxylation of some associated silanol groups on the external surface of the diatomite [33]. In the DTA curve, between 830°C and 1,000°C was observed endothermic-exothermic peak system: solid phase structural decomposition and crystallization which was seen by 1.4% weight loss from TG curve. The diatom frustule decomposition may begin in the range of 900°C–1,000°C because it exhibits an evident decrease in the specific surface area of diatomite [34].

The X-ray powder diffraction results of D_R and thermally treatment diatomite all samples are shown in Fig. 5. The diffraction spectrogram indicates that the natural diatomite consists mainly of quartz (2θ ~27°), amorphous material, smectite group clay minerals, mixed layered clay mineral, feldspar group minerals, illite-mica group minerals, calcite, a very small amount dolomite and kaolinite group minerals. The amorphous region is observed especially quartz and calcite peaks. The XRD pattern of D_R is characteristic of one broad peak observed in this figure (2θ range from 16° to 32°) and may be associated with the glass formation of SiO_2. The peak at 21.8 was due to the presence of SiO_2 in the form of cristobalite [25,34].

The value of 2θ ~6° shows that the Caldiran-Van diatomite contains various clay group minerals as the smectite. The position of this peak shifted to right at 300°C, and the position and intensity of this peak remains constant between 400°C and 800°C and disappeared at 900°C. The shifting indicates the collapse of the interlayer spaces after the dehydration of water coordinated to the exchangeable cations is complete. Thermal treatment did not dramatically change the mineral characteristics of diatomite except including clay minerals until 1,000°C, as indicated by the fact that the

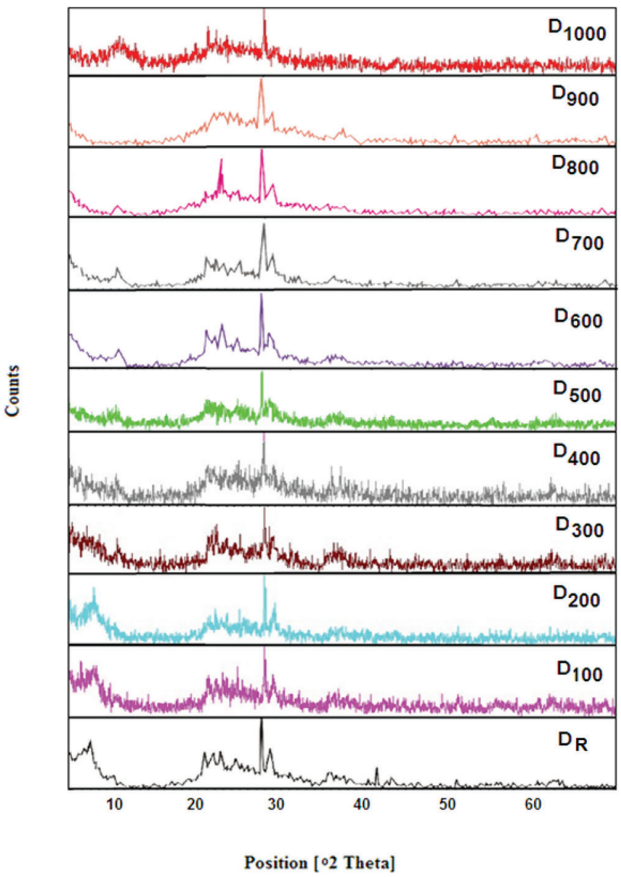

Fig. 5. XRD pattern of the diatomite with different calcination temperature.

XRD patterns of diatomite heated at temperatures lower than 1,000°C remained unchanged. SEM has been a primary tool for characterizing the fundamental physical properties of the adsorbent. It is useful for determining the particle shape and appropriate size distribution of the adsorbent [8]. Scanning electron micrographs of D_R and D_{500} are shown in Figs. 6(a) and 6(b).

The dominant diatom of sample D_R is circular-shaped particles with sizes of 0.005–0.025 mm in clay matrix [20]. It can be inferred from the scanning micrograph that raw diatomite has a large void volume, in addition to its highly porous structure (Fig. 6(a)) [35]. After thermal treatment at 500°C, it consists of some clusters and increases amount of particles as shown in Fig. 6(b).

3.2. Adsorption capacity for heavy metals

It is essential to evaluate the effect of contact time required to reach equilibrium for designing batch adsorption experiments [36]. The amounts of heavy metal ions adsorbed at various time periods (q_t) were calculated via Eq. (1):

$$q_t = \frac{(c_0 - c_t)V}{m} \quad (1)$$

where C_0 is the initial concentration of the metal ions solution; C_t is the concentration of metal ions present in the aqueous

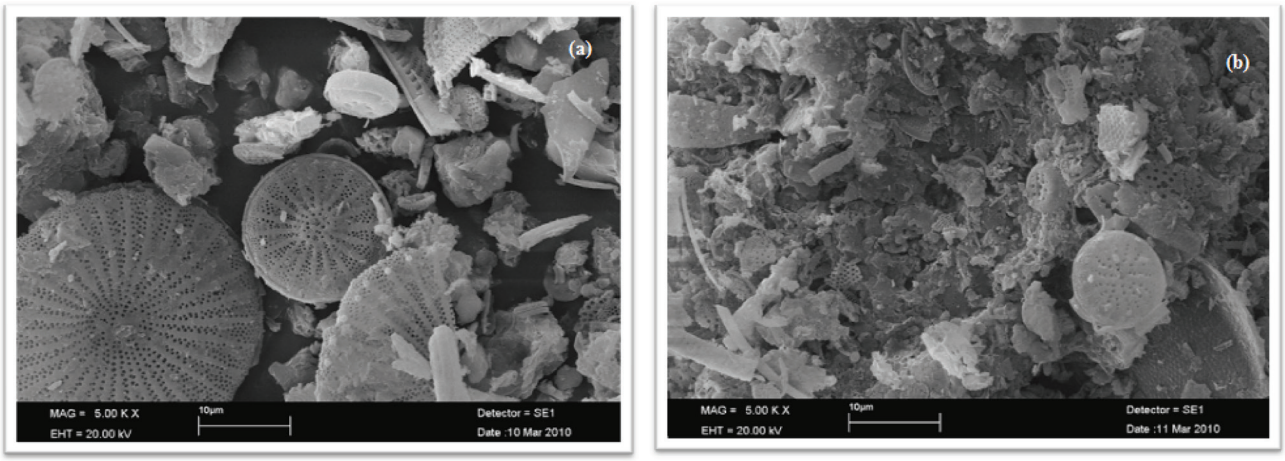

Fig. 6. Typical scanning electron micrographs for (a) D_R and (b) D_{500}.

solution after t min (mg L^{-1}); V is the volume of the solution (L) and m is the mass of adsorbent employed (mg).

The effect of the contact time on the adsorption of Pb(II), Cu(II) and Cd(II) ions onto the D_R and D_{500} samples studied is presented in Fig. 7(a), (b) and (c), where measurements were made over a period of 1–120 min.

As illustrated in Fig. 7, adsorption of metal ions increased with the contact time up to 90 min. From this minute the metal ion adsorption did no longer increase. This explains that the adsorption sites are more at the initial phase, and the metal ions can easily interact with these sites, thereby achieving a higher adsorption rate. The slow adsorption rate was observed in next step because of slower diffusion of solute into the internal of the adsorbent [20]. The amount of metal adsorbed on the examined samples of diatomite generally increases after thermal treatment. The efficiency of these adsorbents showed in Fig. 8. This is ascribed to the fact that diatomite pores are cleaned by applied thermal process, because potential impurities are removed (maybe desorption and volatilization) [18].

The nature of the interaction between the adsorbate and adsorbent, that is, favorable or unfavorable, can be determined from the isotherm shape [35,37]. Generally, metal isotherms were of L-type [38], indicating a high affinity between sorbent and solute [39]. Three isotherm models namely Langmuir (Eq. (3)), Freundlich (Eq. (4)) and Dubinin–Radushkevich (D–R) (Eq. (5)) are used to describe the equilibrium data of lead, copper and cadmium sorption by studied adsorbents (D_R and D_{500}) [23]. The amount of metal adsorbed per gram of the adsorbent at equilibrium (q_e; mg g^{-1}) and the above-mentioned three models are given, respectively, as follows:

$$q_e = \frac{(c_0 - c_e)V}{m} \tag{2}$$

$$q_e = q_{\max} - \frac{q_e}{k_L q_e C_e} \tag{3}$$

$$\ln q_e = \ln k_F + \frac{1}{n}\ln C_e \tag{4}$$

$$In\, q_e = In\, q_{\max} - \beta \cdot \varepsilon^2 \tag{5}$$

$$\varepsilon = RT\, In\left(1 + \frac{1}{c_e}\right) \tag{6}$$

$$E = (2\beta)^{-\frac{1}{2}} \tag{7}$$

where C_e, the equilibrium concentration of adsorbate (mg L^{-1}); C_o is the initial concentration of the metal ions solution; V and m quantities in Eq. (2) have the same meanings as in Eq. (1); $q_{\max}$ is maximum monolayer coverage capacity (mg g^{-1}); and k_L is Langmuir isotherm constant (L mg^{-1}) [40]. k_F is the adsorption capacity constant of the Freundlich model (mg^{1-n} L^n g^{-1}), and n is the adsorption intensity constant of the Freundlich equation. If n = 1 then the partition between the two phases is independent of the concentration. If value of $1/n$ is below one it indicates a normal adsorption. On the other hand, $1/n$ being above one indicates cooperative adsorption [40,41]. β is the constant of D–R isotherm related to adsorption energy (mol^2 kJ^{-2}); ε (Polanyi potential) is determined from Eq. (6). R is gas constant (kJ K^{-1} mol^{-1}), and T' (K) is temperature. The sorption energy E (kJ mol^{-1}) is calculated from Eq. (7) which gives information about physical or chemical characteristics of adsorption. E is between 8 and 16 kJ mol^{-1}, the sorption process follows chemical ion exchange, while for the values of E < 8 kJ mol^{-1}, the sorption process is of a physical nature [20].

The Langmuir constant (k_L) is used to calculate R_L, a dimensionless separation factor given by Eq. (8):

$$R_L = \frac{1}{1 + k_L C_0} \tag{8}$$

where C_0 is the initial metal concentration (mg L^{-1}). The R_L values indicate whether the adsorption is unfavorable (R_L > 1), linear (R_L = 1), favorable (0 < R_L < 1), or irreversible (R_L = 0) [42]. The Langmuir model assumes that the adsorbent surface has sites of identical energy and that each adsorbate molecule is located at a single site; hence, it predicts the formation of a monolayer of the adsorbate on the adsorbent surface [42].

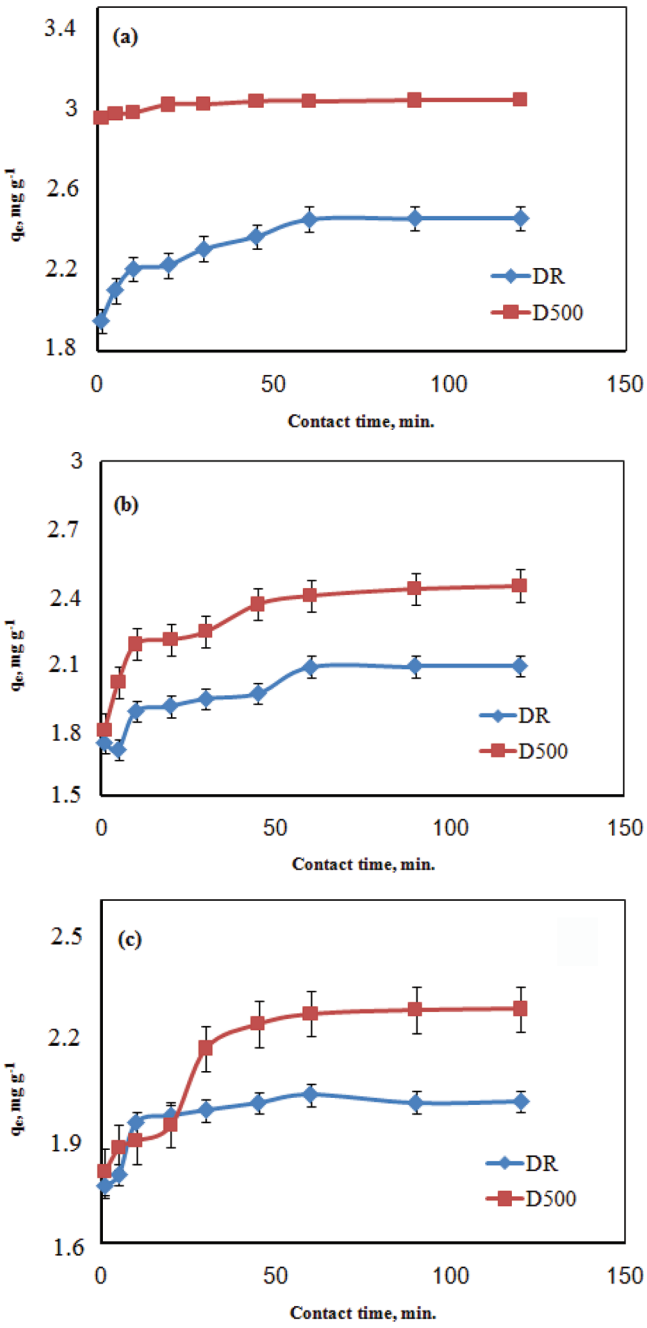

Fig. 7. Effect of contact time on adsorption amount of (a) Pb(II), (b) Cu(II) and (c) Cd(II) on D_R and D_{500}. Error bars represent standard deviation.

The Freundlich equation is an isotherm model representing the adsorbent surface as heterogeneous [41]. The D–R isotherm is generally applied to express the adsorption mechanism with a Gaussian energy distribution onto a heterogeneous surface [40]. To further understand adsorption of Pb(II), Cu(II) and Cd(II) onto natural and thermally modified diatomite, adsorption isotherms of metal solutions at pH 4.0 were evaluated. As mentioned above, the adsorption isotherms for both adsorbent (raw and modified diatomite) fit Langmuir isotherm with high correlation coefficients for all systems studied. This supports

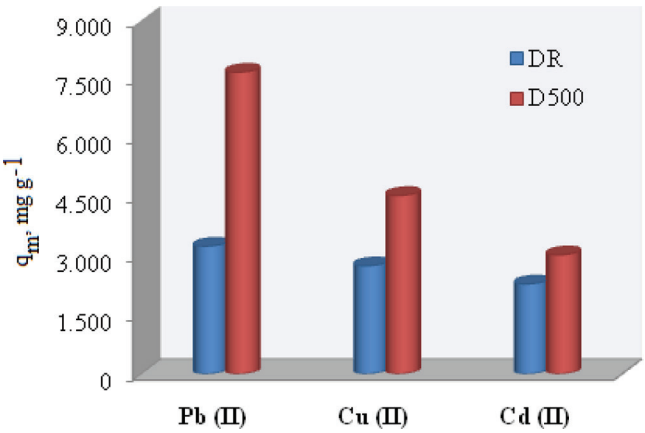

Fig. 8. The maximum monolayer coverage capacity of each metal ion per mass of the adsorbate used (mg g^{-1}) (q_{max}) for each of the two diatomite samples examined. (in 30 mg L^{-1} initial metal ion concentrations at 298 K).

the theory that the number of sites on the diatomite surface is limited and the heavy metals form a monomolecular layer on the surface at maximum capacity [35]. Fig. 9 presents linear plots of three isotherm models for Pb(II), Cu(II) and Cd(II) adsorption onto D_R and D_{500} samples [41].

The parameters or constants of Langmuir, Freundlich and D–R isotherms are shown in Table 1.

The Langmuir monolayer adsorption capacities, q_m, of Pb(II), Cu(II) and Cd(II) ions were estimated to be 3.253, 2.754 and 2.292 mg g^{-1}, respectively, for D_R and 7.686, 4.545 and 3.033 mg g^{-1} for D_{500}, respectively, at 298 K. Adsorption of heavy metals onto D_R and D_{500} decreases in the order: Pb(II) > Cu(II) > Cd(II). The superior adsorption of lead ions onto raw and modified diatomite could be attributed to the electronegativity of the metal ions [35]. The higher ionic radius and higher electronegativity of lead (2.33) could explain that lead is more favorable for adsorption than copper (1.90) and cadmium (1.69) [2]. The ionic radii of the lead, copper and cadmium are 1.2, 0.72 and 0.97 Å, respectively, which were very small to keep in the mesopores. Consequently, the more enhance in metal crystal radius, the more retention in the mesopores and more adsorption could be expected as a result [2]. The n values between 1 and 10 represent favorable adsorption [39]. From Table 1, the n values were >1, which indicated a favorable adsorption of heavy metal ions onto D_R and D_{500} samples. The E values were calculated from D-R equation as 0.980, 0.442 and 1.111 kJ mol^{-1} for adsorption of Pb(II), Cu(II) and Cd(II) ions onto D_R, respectively, while values of 0.780, 0.342 and 1.018 kJ mol^{-1} are obtained for D_{500}. Since these values are lower than 8 kJ mol^{-1}, it is very likely that lead, copper and cadmium adsorption on D_R and D_{500} is physical in nature.

3.3. Sorption kinetics

Kinetic models, namely pseudo-first-order (Eq. 9), pseudo-second-order (Eq. 10) and intraparticle diffusion model (Eq. 11), are used to determine the adsorption kinetics of lead, copper and cadmium ions onto the D_R and D_{500}.

$$In\,(q_e - q_t) = In\,q_e - k_1\,t \tag{9}$$

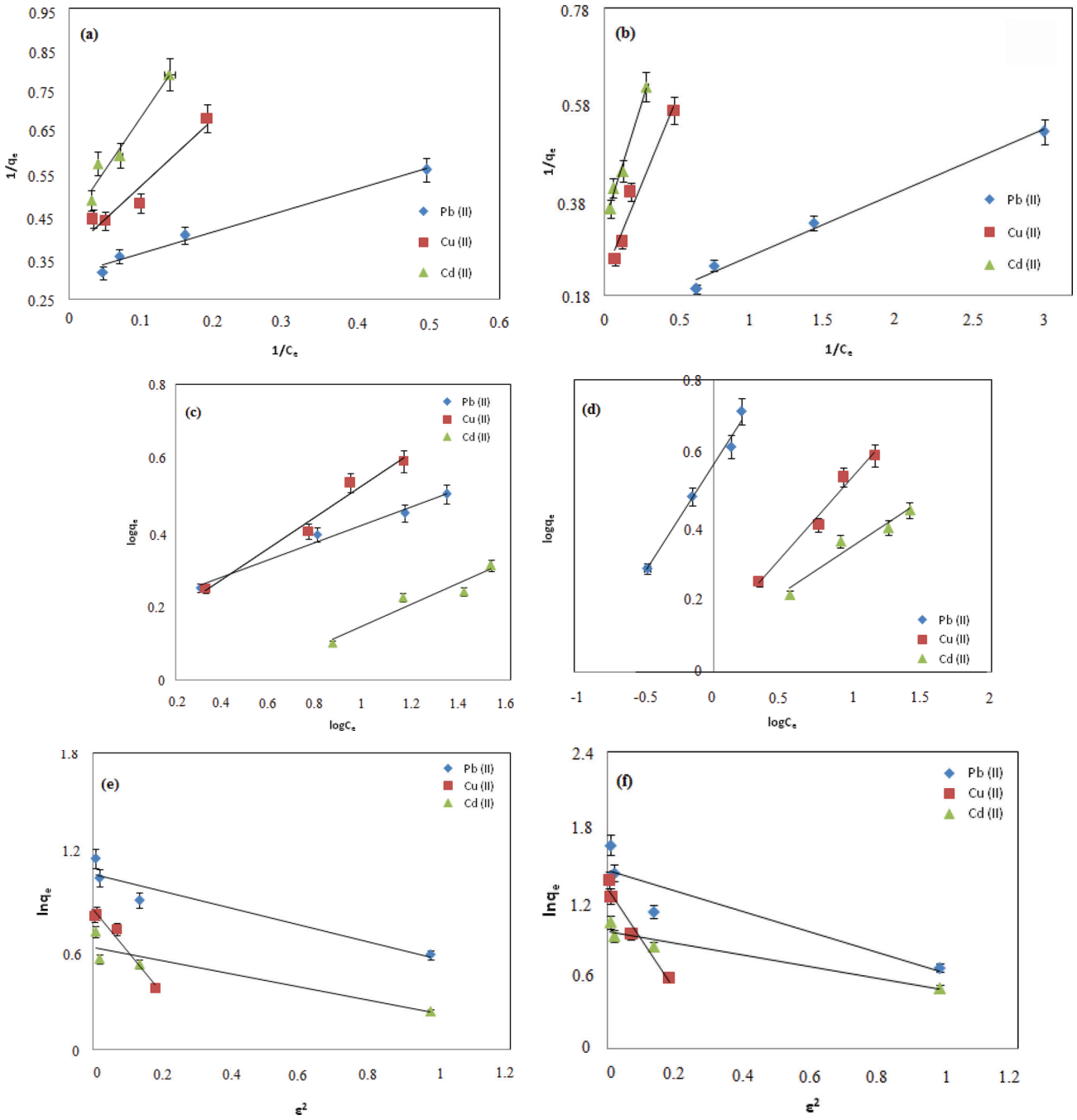

Fig. 9. Langmuir adsorption isotherm of Pb(II), Cu(II) and Cd(II) on (a) D_R and (b) D_{500}; Freundlich adsorption isotherm of Pb(II), Cu(II) and Cd(II) on (c) D_R and (d) D_{500}; and D–R adsorption isotherm of Pb(II), Cu(II) and Cd(II) on (e) D_R and (f) D_{500} (in 30 mg L^{-1} initial metal ion concentrations at 298 K). Error bars represent standard deviation.

$$\frac{t}{q_t} = \frac{1}{k_2 \cdot q_e^2} + \frac{1}{q_e} \cdot t \tag{10}$$

$$q_t = k_i\, t^{1/2} + c \tag{11}$$

where q_t and q_e (mg g^{-1}) are the adsorption capacity at time t and equilibrium time, respectively, and k_1 (min^{-1}) is the pseudo-first-order model rate constant; k_2 (g mg^{-1} min^{-1}) is the pseudo-second-order model adsorption rate constant; and k_i (mg g^{-1} $min^{1/2}$) is the rate constant for intraparticle diffusion [23,36,43]. The value of C gives an idea of the thickness of boundary layer; the larger the intercept the greater the boundary layer effect [36]. Linear lines obtained from the variation of t/q_t against t according to pseudo-second-order model. Figs. 10(a) and 10(b) show the application of the pseudo-second-order model to the data as plots of t/q_t vs. t [44].

Table 1
Langmuir, Freundlich and D–R isotherm constants for the adsorption of Pb(II), Cu(II) and Cd(II) onto D_R and D_{500} in 30 mg L^{-1} initial metal ion concentrations at 298 K

Parameters	D_R			D_{500}		
	Pb(II)	Cu(II)	Cd(II)	Pb(II)	Cu(II)	Cd(II)
Langmuir model						
q_m (mg g^{-1})	3.253	2.754	2.292	7.686	4.545	3.033
k_L	0.592	0.227	0.173	0.988	0.293	0.332
R_L	0.046	0.303	0.085	0.500	0.0076	0.006
R^2	0.9832	0.9374	0.9472	0.9882	0.9564	0.9854
Freundlich model						
k_F	1.534	1.069	0.740	2.376	1.265	1.235
n	4.201	4.120	3.522	1.660	2.314	3.957
R^2	0.9858	0.8032	0.9169	0.9865	0.9767	0.9400
D–R model						
β (mol^2 kJ^{-2})	0.520	2.550	0.405	0.851	0.780	0.482
q_{max} (mg g^{-1})	2.913	2.356	1.859	4.254	3.691	2.580
E (kJ mol^{-1})	0.980	0.442	1.111	0.780	0.342	1.018
R^2	0.9047	0.9689	0.8686	0.8308	0.9598	0.9342

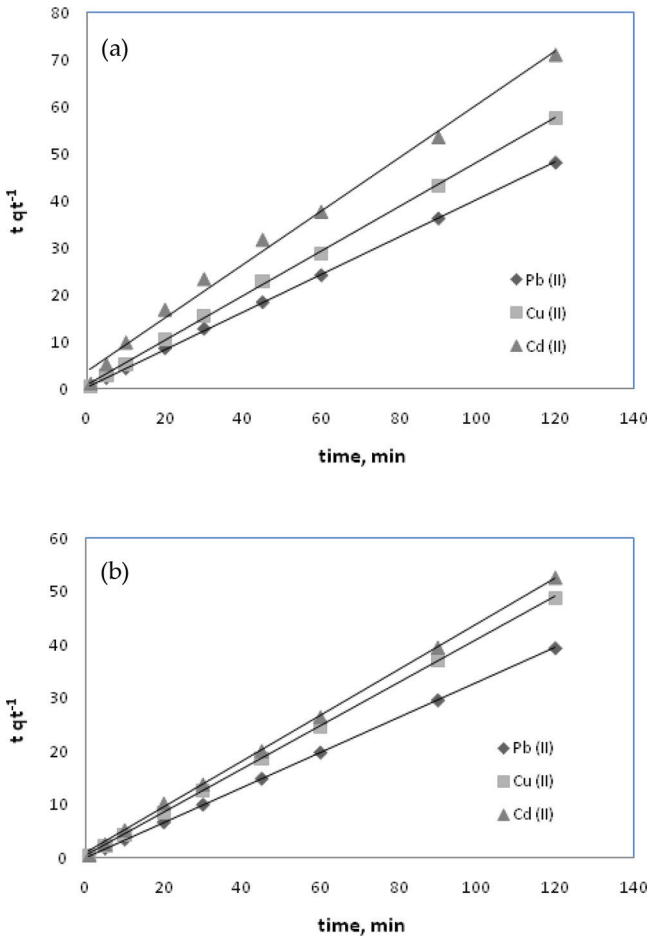

Fig. 10. Pseudo-second-order adsorption kinetics of Pb(II), Cu(II) and Cd(II) on (a) D_R and (b) D_{500} in 30 mg L^{-1} initial metal ion concentrations at 298 K.

Adsorption process is a multi-step process involving transport of solute molecules from the aqueous phase to the surface of the solid particles. This is followed by the diffusion of the solute molecules into the interior part of the pores, which is likely to be a slow process; therefore, it is called the rate determining step [36]. The intraparticle diffusion plot is the plot of amount sorbed per unit weight of sorbent, q_t (mg g^{-1}) vs. square root of time, $t^{1/2}$, is shown in Fig. 11(a) (D_R) and 11(b) (D_{500}) for initial metal ions concentration of 30 mg L^{-1} at 298 K [20].

Figs. 11(a) and 11(b) indicate that the adsorption plots non-linear over the whole time range and can be divided into multi-linear regions which verify the multi stages of adsorption. The first stage is attributed to the boundary layer diffusion of metal ions, and the second stage is due to the intraparticle diffusion effects [1,35,36]. If the intraparticle diffusion is the only rate-limiting step, it is essential for the q_t vs. $t^{1/2}$ plots to go through the origin. On the other hand, these plots (Figs. 11(a) and 11(b)) not only fitted with a straight line passing through the origin but also with poor linear regression coefficients (R^2) indicating the inadaptability of this model, and the intraparticle diffusion was not merely the rate-controlling step [20]. All the kinetic parameters obtained employing the pseudo-first-order, pseudo-second-order and intraparticle diffusion models are listed in Tables 2(a) and (b). The parameters of sorption kinetic are calculated from the corresponding slopes and intercepts [18].

It will be seen from Tables 2(a) and (b), the values of q_e calculated from the pseudo-first-order model are not consistent with the experimental values of q_e. It seems that the kinetics of Pb(II), Cu(II) and Cd(II) adsorption on D_R and D_{500} samples followed the pseudo-second-order model, providing high correlation coefficient (R^2). In addition, the q_e values calculated from the pseudo-second-order model are match with q_e experimental results. Obviously, the thermal treatment of diatomite at 500°C not only increased the adsorption capacity of the material but also accelerated the adsorption kinetic

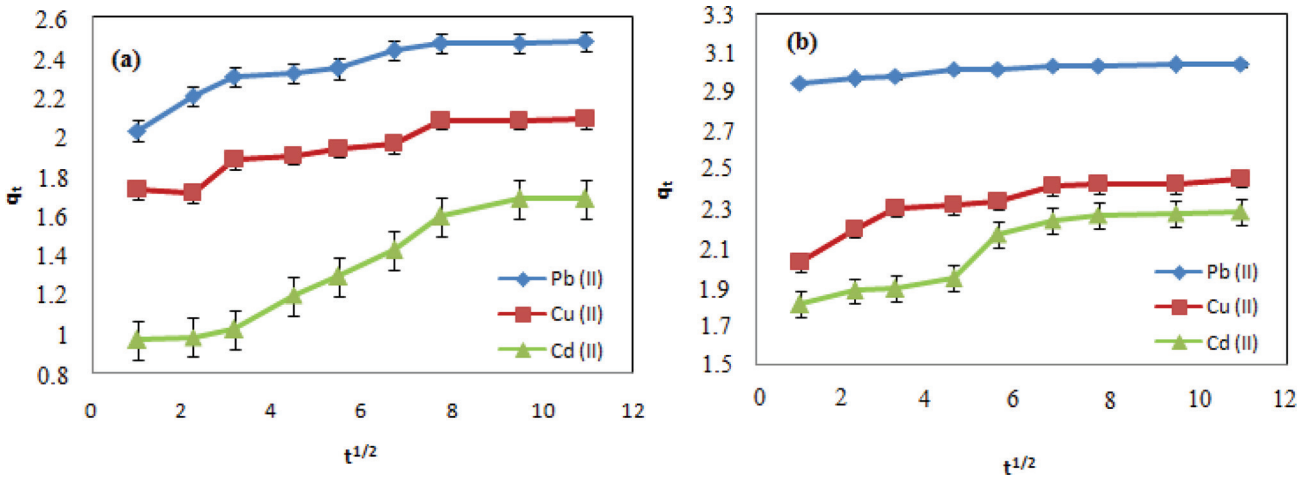

Fig. 11. Intraparticle diffusion plots of adsorption of Pb(II), Cu(II) and Cd(II) on (a) D_R and (b) D_{500} in 30 mg L^{-1} initial metal ion concentrations at 298 K. Error bars represent standard deviation.

Table 2a
Raw diatomite: Intraparticle diffusion, pseudo-first-order and pseudo-second-order kinetic parameters of Pb(II), Cu(II) and Cd(II) ions on D_R in various initial metal ions concentrations at 298 K

		Pseudo-first-order			Pseudo-second-order			Intraparticle diffusion model		
Metal ions	C_0 (mg L^{-1})	q_e (exp) (mg g^{-1})	q_e (cal) (mg g^{-1})	k_1 (min^{-1})	R^2	q_e (cal) (mg g^{-1})	k_2 (g mg^{-1} min^{-1})	R^2	k_i	R^2
Pb(II)	10	0.917	0.021	0.082	0.9312	0.920	4.081	0.9999	0.001	0.9054
	20	1.781	0.051	0.140	0.8880	1.388	0.398	0.9994	0.012	0.9486
	30	2.479	0.112	0.110	0.9102	2.506	0.408	0.9998	0.041	0.8281
	45	2.835	0.610	0.142	0.7943	2.873	0.235	0.9996	0.093	0.5447
	60	3.194	3.410	0.160	0.7048	3.424	0.088	0.9966	0.081	0.9130
Cu(II)	10	0.815	0.005	0.036	0.9416	0.836	0.331	0.9966	0.021	0.9043
	20	1.459	0.102	0.016	0.8598	1.469	0.724	0.9998	0.027	0.8798
	30	2.081	0.309	0.013	0.8170	2.105	0.311	0.9994	0.039	0.8865
	45	2.284	0.622	0.032	0.8851	2.652	0.133	0.9983	0.080	0.9386
	60	2.269	1.608	0.002	0.9766	3.106	0.067	0.9965	0.126	0.9536
Cd(II)	10	0.590	0.003	0.483	0.8987	0.606	1.351	0.9995	0.006	0.9691
	20	1.263	0.623	0.036	0.5273	1.287	0.420	0.9989	0.027	0.8438
	30	1.680	0.493	0.053	0.9474	1.762	0.560	0.9931	0.086	0.9579
	45	1.736	0.769	0.055	0.9861	1.864	0.684	0.9891	0.103	0.9451
	60	2.048	1.254	0.154	0.9065	2.173	0.127	0.9977	0.073	0.9374

rate for Pb(II) and Cu(II) ions [4]. On the contrary, it is difficult to do this comment for Cd(II) ion adsorption kinetic rate constant (k_2).

3.4. Sorption thermodynamics

To measure the thermodynamic parameters, the experiments were conducted at different temperatures in the range of 298–328 K for Pb(II), Cu(II) and Cd(II) ions adsorption [45]. Thermodynamic parameters including the changes in standard Gibb's free energy ΔG^0 (kJ mol^{-1}), enthalpy ΔH^0 (kJ mol^{-1}) and entropy ΔS^0 (J mol^{-1} K^{-1}) can be calculated in order to illustrate the thermodynamic behavior of adsorption process [46]:

$$K_d = \frac{(C_0 - C_e)V / m}{C_e} \quad (12)$$

Table 2b
500°C diatomite: Intraparticle diffusion, pseudo-first-order and pseudo-second-order kinetic parameters of Pb(II), Cu(II) and Cd(II) ions on D_{500} in different initial metal ions concentrations at 298 K

Metal ions	C_0 (mg L^{-1})	Pseudo-first-order			Pseudo-second- order			Intraparticle diffusion model		
		q_e (exp) (mg g^{-1})	q_e (cal) (mg g^{-1})	k_1 (min^{-1})	R^2	q_e (cal) (mg g^{-1})	k_2 (gm g^{-1} min^{-1})	R^2	k_i	R^2
Pb(II)	10	0.915	0.001	0.084	0.9312	0.925	6.588	1.0000	0.001	0.9059
	20	1.920	0.006	0.220	0.9679	1.941	4.839	1.0000	0.004	0.9125
	30	3.028	0.007	0.169	0.9786	3.046	2.103	1.0000	0.009	0.8471
	45	4.144	0.114	0.186	0.9155	3.584	0.635	1.0000	0.030	0.8518
	60	5.191	0.105	0.102	0.9724	5.299	0.387	1.0000	0.036	0.9382
Cu(II)	10	0.903	0.020	0.179	0.9070	0.904	7.954	1.0000	0.002	0.8433
	20	1.799	0.015	0.193	0.7668	1.814	0.921	0.9999	0.012	0.9598
	30	2.529	0.061	0.138	0.8947	2.461	0.503	0.9999	0.020	0.5788
	45	3.425	4.688	0.172	0.7497	3.532	0.055	0.9937	0.012	0.7015
	60	3.920	4.446	0.080	0.7863	5.319	0.392	1.0000	0.013	0.8699
Cd(II)	10	0.905	0.046	0.097	0.9911	0.921	0.499	0.9993	0.023	0.9442
	20	1.629	0.691	0.161	0.9220	1.661	0.303	0.9997	0.057	0.8105
	30	2.281	0.441	0.151	0.9508	2.318	0.247	0.9994	0.055	0.8713
	45	2.484	0.069	0.057	0.8335	2.595	0.080	0.9889	0.104	0.9548
	60	2.779	0.085	0.002	0.8326	2.793	0.411	0.9997	0.023	0.9297

$$InK_d = \frac{\Delta S^\circ}{R} - \frac{\Delta H^\circ}{R}\frac{1}{T} \quad (13)$$

$$\Delta H^0 = \Delta G^0 + T\Delta S^0 \quad (14)$$

where K_d is the coefficient for the distribution of the solute between the adsorbent and the solution at equilibrium (q_e/C_e), which can be obtained from Eq. (12) for different temperatures; R (8.314 J mol^{-1} K^{-1}) is the ideal gas constant; T is the temperature in Kelvin (K) [44]. The values of standard enthalpy change (ΔH^0) and entropy change (ΔS^0) were calculated from the slope and intercept of the plot lnK_d vs. $1/T$ as required by Eq. (13). Free energy changes (ΔG^0) of specific adsorption are calculated from Eq. (14). The calculated values of thermodynamic parameters are reported in Table 3.

As observed, the adsorption of Pb(II), Cu(II) and Cd(II) by D_R and D_{500} was spontaneous and feasible with the negative values of ΔG^0. It is known that ΔG^0 values up to –20 kJ mol^{-1} show electrostatic interaction between adsorption sites and the metal ion (physical adsorption), while more negative values around –40 kJ mol^{-1} or higher involve electron sharing (chemical adsorption). These values increased in absolute value when T increased, showing that the adsorption was more spontaneous at higher temperature [47]. A positive value of ΔH^0 is indicated that the adsorption process is endothermic in nature. In general, the enthalpy change due to chemisorption (>40 kJ mol^{-1}) is considerably larger than that of physisorption (<40 kJ mol^{-1}) [44,48]. The lower order of magnitude of ΔH^0 (see in Table 3) confirmed the physisorption mechanism of Pb(II), Cu(II) and Cd(II) ions onto D_R and D_{500}. Physical adsorption involves relatively weak intermolecular forces such as van der Waals forces, electrostatic interaction as well as hydrogen bonding [44]. A positive value of ΔS^0 revealed an increased randomness between solid-solution interfaces during the adsorption of lead, copper and cadmium ions on D_R and D_{500} [45]. This positive value also suggested the affinity heavy metal ions toward the adsorbent particles and an increased degree of freedom of the adsorbed metal ions [48].

4. Conclusion

The raw and thermally modified diatomite at 500°C was tested for the adsorption of Pb(II), Cu(II) and Cd(II) from aqueous solutions. Improvement in diatomite performance following modification by thermal treatment could be attributed to an increase of mesopores in structure that it is suitable for adsorption and cleaning of pores by burning of organic impurities. The adsorption isotherms of heavy metals onto raw and calcined diatomite were examined by Langmuir, Freundlich and D–R models. It is understood that the Langmuir is the best one, indicating that the number of adsorption sites on the adsorbent surface is limited and the lead, copper and cadmium ions form a monomolecular layer on the surface at maximum capacity. The values of the adsorption energy (see in Table 1; E < 8 kJ mol^{-1}) calculated from the D–R adsorption isotherm showed that the mechanism for the adsorption of Pb(II), Cu(II) and Cd(II) ions onto the diatomite examined involved a combination

Table 3
Values of thermodynamic parameters for the adsorption of Pb(II), Cu(II) and Cd(II) ions onto D_R and D_{500}

Adsorbent	Metal ions	C_0 (mg L^{-1})	ΔH^0 (kJ mol^{-1})	ΔS^0 (J $mol^{-1} K^{-1}$)			ΔG^0 (kJ mol^{-1})	
					298 K	308 K	318 K	328 K
D_R	Pb(II)	10	21.159	98	–8.223	–9.209	–10.19	–11.182
		20	17.517	80	–6.352	–7.153	–7.954	–8.755
		30	3.700	16	–1.068	–1.228	–1.388	–1.548
		45	2.702	15	–1.768	–1.918	–2.068	–2.218
		60	6.102	64	–12.970	–13.61	–14.250	–14.890
	Cu(II)	10	0.266	14	–3.906	–4.046	–4.186	–4.326
		20	1.895	2.0	–1.299	–1.279	–1.259	–1.239
		30	0.557	7.0	–1.752	–1.830	–1.907	–1.985
		45	0.326	12	–3.250	–3.370	–3.490	–3.610
		60	1.430	5.0	–0.600	–0.110	–0.160	–0.210
	Cd(II)	10	2.574	13	–1.300	–1.430	–1.560	–1.690
		20	3.032	17	–2.034	–2.204	–2.374	–2.544
		30	4.280	22	–2.276	–2.496	–2.716	–2.936
		45	1.181	32	–8.355	–8.675	–8.995	–9.315
		60	1.664	16	–3.104	–3.264	–3.424	–3.584
					298 K	308 K	318 K	328 K
D_{500}	Pb(II)	10	1.305	29	–7.337	–7.627	–7.917	–8.207
		20	19.936	83	–4.798	–5.628	–6.458	–7.288
		30	22.921	91	–4.197	–5.107	–6.017	–6.927
		45	18.390	83	–6.344	–7.174	–8.004	–8.834
		60	14.374	68	–5.890	–6.570	–7.250	–7.930
	Cu(II)	10	27.419	117	–7.447	–8.617	–9.787	–10.957
		20	24.559	108	–7.625	–8.705	–9.785	–10.865
		30	12.022	66	–7.646	–8.306	–8.966	–9.626
		45	21.687	84	–3.345	–4.185	–5.025	–5.865
		60	5.645	26	–2.103	–2.363	–2.623	–2.883
	Cd(II)	10	5.753	32	–3.783	–4.103	–4.423	–4.743
		20	3.384	22	–3.172	–3.392	–3.612	–3.832
		30	2.904	23	–3.950	–4.180	–4.410	–4.640
		45	2.938	18	–2.425	–2.605	–2.785	–2.965
		60	1.160	11	–2.118	–2.228	–2.338	–2.448

of electrostatic interaction and physical sorption. Since the values of adsorption enthalpy for two diatomite samples were less than 40 kJ mol^{-1}, this confirms that the sorption process was controlled by a physical mechanism rather than a chemical mechanism in all the studied cases. The kinetic studies of heavy metals onto raw and calcined diatomite reveal that the adsorption behavior is better described by the pseudo-second-order model than the pseudo-first-order model. In addition, experiments obviously show that adsorption of Pb(II), Cu(II) and Cd(II) ions on diatomite samples is a multi-step process concerning transport of these ions from the aqueous solution to the surface of the solid particles. In this study, for the three metals, the adsorption capacity followed the order of Pb > Cu > Cd, which may be attributed to their different adsorption affinities. The adsorption affinities are associated with their properties such as ionic radii and electronegativity. However, that the adsorption capacity for heavy metals is extremely dependent on the experimental conditions, for example, pH, solution temperature, initial metal ion concentration

and adsorbent particle size [22]. These results show that the Pb(II), Cu(II) and Cd(II) ions were possibly adsorbed onto negatively charged sites (hydroxyl groups) on the adsorbent surfaces via ion-exchange reactions under the experimental conditions employed in the present work.

Acknowledgments

This study was produced from PhD thesis of Eda Gokirmak Sogut. Financial support was provided by the Research Fund of Yüzüncü Yıl University, Van, Turkey (Project number: 2010-FBE-D147).

References

[1] S. Sungworawongpana, S. Pengprecha, Calcination effect of diatomite to chromate adsorption, Procedia Eng., 8 (2011) 53–57.
[2] S.S. Ibrahim, H.S. Ibrahim, N.S. Ammar, H.H. Abdel Ghafar, T.S. Jamil, M. Farahat, Applicability of Egyptian diatomite for uptake of heavy metals, Desalin. Water Treat., 51 (2013) 2343–2350.
[3] A.P.S. Reza, A.M. Hasan, J.J. Ahmad, F. Zohreh, T. Jafar, The effect of acid and thermal treatment on a natural diatomite, Chem. J., 1 (2015) 144–150.
[4] M. Aivalioti, P. Papoulias, A. Kousaiti, E. Gidarakos, Adsorption of BTEX, MTBE and TAME on natural and modified diatomite, J. Hazard. Mater., 207 (2012) 117–127.
[5] S.C. Ma, Z.G. Wang, J.L. Zhang, D.H. Sun, G.X. Liu, Detection analysis of surface hydroxyl active sites and simulation calculation of the surface dissociation constants of aqueous diatomite suspensions, Appl. Surf. Sci., 327 (2015) 453–461.
[6] L.T. Zhuravlev, The surface chemistry of amorphous silica. Zhuravlev model, Colloids Surf., A, 173 (2000) 1–38.
[7] T.H. Muster, C.A. Prestige, R.A. Hayes, Water adsorption kinetic and contact angles of silica particles, Colloids Surf. A, 176 (2001) 253–266.
[8] M.A.M. Khraisheh, S.J. Al-Ghouti, M.N. Ahmad, Effect of OH and silanol groups in the removal of dyes from aqueous solution using diatomite, Water Res., 39 (2005) 922–932.
[9] N. Ediz, İ. Bentli, İ. Tatar, Improvement in filtration characteristics of diatomite by calcinations, Int. J. Miner. Process., 94 (2010) 129–134.
[10] F. Akhtar, Y. Rehman, L. Bergström, A study of the sintering of diatomaceous earth to produce porous ceramic monoliths with bimodal porosity and high strength, Powder Technol. 201 (2010) 253–257.
[11] B. Bahramian, F.D. Ardejani, V. Mirkhani, K. Badii, Diatomite-supported manganese Schiff base: an efficient catalyst for oxidation of hydrocarbons, Appl. Catal., A, 345 (2008) 97–103.
[12] A.C. Aydin, R. Gu, Influence of volcanic originated natural materials as additive on the setting time and some mechanical properties of concrete, Constr. Build. Mater., 21 (2007) 1277–1281.
[13] M.A.M. Khraisheh, Y.S. Al-Degs, W.A.M. Mcminn, Remediation of wastewater containing heavy metals using raw and modified diatomite, Chem. Eng. J., 99 (2004) 177–184.
[14] M.A. Al-Ghouti, M.A.M. Khraisheh, M. Tutuji, Flow injection potentiometric stripping analysis for study of adsorption of heavy metal ions onto modified diatomite, Chem. Eng. J., 104 (2004) 83–91.
[15] P. Srivastava, B. Singh, M. Angove, Competitive adsorption behavior of heavy metals on kaolinite, J. Colloid Interface Sci., 290 (2005) 28–38.
[16] A.F.D. Namor, A.E. Gamouz, S. Frangie, V. Martinez, L. Valiente, O.A. Webb, Turning the volume down on heavy metals using tuned diatomite. A review of diatomite and modified diatomite for the extraction of heavy metals from water, J. Hazard. Mater., 241 (2012) 14–31.
[17] J.X. Lin, S.L. Zhan, M.H. Fang, X.Q. Qian, The adsorption of dyes from aqueous solution using diatomite, J. Porous Mater., 14 (2007) 449–455.
[18] M. Aivalioti, I. Vamvasakis, E. Gidarakos, BTEX and MTBE adsorption onto raw and thermally modified diatomite, J. Hazard. Mater., 178 (2010) 136–143.
[19] P. Yuan, D. Yang, Z.Y. Lin, H.P. He, X.Y. Wen, L.J. Wang, F. Deng, Influences of pretreatment temperature on the surface silylation of diatomaceous amorphous silica with trimethylchlorosilane, J. Non-Cryst. Solids, 352 (2006) 3762–3771.
[20] N. Caliskan, A.R. Kul, S. Alkan, E.G. Sogut, I. Alacabey, Adsorption of zinc(II) on diatomite and manganese-oxide-modified diatomite: a kinetic and equilibrium study, J. Hazard. Mater., 193 (2011) 27–36.
[21] Z. Sun, Y. Zhanga, S. Zhenga, Y. Park, R.L. Frostb, Preparation and thermal energy storage properties of paraffin/calcined diatomite composites as form-stable phase change materials, Thermochim. Acta, 558 (2013) 16–21.
[22] S. Yusan, C. Gok, S. Erenturk, S. Aytas, Adsorptive removal of thorium (IV) using calcined and flux calcined diatomite from Turkey: Evaluation of equilibrium, kinetic and thermodynamic data, Appl. Clay. Sci., 67 (2012) 106–116.
[23] M.D. Irani, M. Amjadi, A.M.D. Mousavian, Comparative study of lead sorption onto natural perlite, dolomite and diatomite, Chem. Eng. J., 178 (2011) 317–323.
[24] B.A. Morrow, I.D. Gay, Infrared and NMR Characterization of the Silica Surface, In: E. Papirer, *Adsorption on Silica Surfaces*, Marcel Dekker Inc., New York Basel, 2000, pp. 9–35.
[25] J.F. Cano, R.L. Ramos, E.P. Ortega, J.M. Barron, Adsorption of heavy metals on diatomite: mechanism and effect of operating variables, Adsorpt. Sci. Technol., 31 (2013) 275–292.
[26] M.A. Karakassides, D. Gournis, D. Petridis, An infrared reflectance study of Si–O vibrations in thermally treated alkali-saturated montmorillonites, Clay Miner., 34 (1999) 429–429.
[27] W. Zhi-Ying, Z. Li-Ping, Y. Yu-Xiang, Structural investigation of some important Chinese diatomites, Glass Phys. and Chem, 35 (2009) 673–679.
[28] E. Pretsch, P. Buhlmann, C. Affolter, Structure Determination of Organic Compounds Tables of Spectral Data, Third Completely Revised and Enlarged English Edition, Springer-Verlag, Berlin, Heidelberg, 2000.
[29] P. Yuan, D.Q. Wu, H.P. He, Z.Y. Lin, The hydroxyl species and acid sites on diatomite surface: a combined IR and Raman study, Appl. Surf. Sci., 227 (2004) 30–39.
[30] N.G. Yaroslavsky, Dissertation, Cand. Phys.-Math. Sci., GOI, Leningrad (1948).
[31] U. İpekoğlu, Z. Mete, Determination of the properties of various diatomite deposits within Aegean region of Turkey, Geologija, 33 (1990) 447–459.
[32] W. Fuya, Z. Huifen, F. Huang, C.Guoxi, W. Deqiang, H. Hongping, A mineralogical study of diatomite in Leizhou Peninsula, Chin. J. Geochem., 14 (1995) 140–151.
[33] A. Chaisena, K. Rangsriwatananon, Effects of thermal and acid treatments on some physico-chemical properties of Lampang diatomite, Suranaree J. Sci. Technol., 11 (2004) 289–299.
[34] P. Yuan, D. Liu, D.Y. Tan, K.K. Liu, H.G. Yu, Y.H. Zhong, A.H. Yuan, et al., Surface silylation of mesoporous/macroporous diatomite (diatomaceous earth) and its function in Cu(II) adsorption: the effects of heating pretreatment, Microporous Mesoporous Mater., 170 (2013) 9–19.
[35] M.A.M. Khraisheh, Y. Al-Deges, W. McMinn, Remediation of wastewater containing heavy metals using raw and modified diatomite, Chem. Eng. J., 99 (2004) 177–184.
[36] O.S. Bello, Adsorptive removal of malachite green with activated carbon prepared from oil palm fruit fibre by KOH activation and CO_2 gasification, S. Afr. J. Chem., 66 (2013) 32–41.
[37] M. Sljivic, I. Smiciklas, S. Pejanovic, I. Plecas, Comparative study of Cu^{2+} adsorption on a zeolite, a clay and a diatomite from Serbia, Appl. Clay Sci., 43 (2009) 33–40.
[38] C.H. Giles, D. Smith, A. Huitson, A general treatment and classification of the solute adsorption isotherms-I. Theoretical, J. Colloid Interface Sci., 47 (1974) 755–765.

[39] B. Anna, M. Kleopas, S. Constantine, F. Anestis, B. Maria, Adsorption of Cd(II), Cu(II), Ni(II) and Pb(II) onto natural bentonite: study in mono- and multi-metal systems, Environ. Earth Sci., 73 (2015) 5435–5444.
[40] A.O. Dada, A.P. Olalekan, A.M. Olatunya, O. Dada, Langmuir, Freundlich, Temkin and Dubinin–Radushkevich isotherms studies of equilibrium sorption of Zn2+ unto phosphoric acid modified rice husk, IOSR-JAC, 3 (2012) 38–45.
[41] T.B. Musso, M.E. Parolo, G. Pettinari, F.M. Francisca, Copper and zinc adsorption capacity of three different clay liner materials from Argentina, J. Environ. Manage., 146 (2014) 50–58.
[42] R. Laus, V.T. Fávere, Competitive adsorption of Cu(II) and Cd(II) ions by chitosan crosslinked with epichlorohydrin–triphosphate, Bioresour. Technol., 102 (2011) 8769–8776.
[43] F. Qin, B. Wen, X.Q. Shan, Mechanisms of competitive adsorption of Pb, Cu, and Cd on peat, Environ. Pollut., 144 (2006) 669–680.
[44] A.R. Kul, N. Caliskan, Equilibrium and kinetic studies of the adsorption of Zn(II) ions onto natural and activated kaolinites, Adsorpt. Sci. Technol. 27 (2009) 85–105.
[45] M.A. Hossain, H.H. Ngo, W.S. Guo, T. Setiadi, Adsorption and desorption of copper(II) ions onto garden grass, Bioresour. Technol., 121 (2012) 386–395.
[46] J.M. Smith, H.C. Van Ness, Introduction to Chemical Engineering Thermodynamics, McGraw-Hill, New York, 1987.
[47] P. Miretzky, C. Munoz, E.C. Uriza, Cd^{2+} adsorption on alkaline-pretreated diatomaceous earth: equilibrium and thermodynamic studies, Environ. Chem. Lett., 9 (2011) 55–63.
[48] N. Sivarajasekar, R. Baskar, Adsorption of basic magenta II onto H_2SO_4 activated immature Gossypium hirsutum seeds: kinetics, isotherms, mass transfer, thermodynamics and process design, Arabian J. Chem., 20 (2014) 2699–2709.